11713

Heterovalent Clusters: $Ln_4Se(SePh)_8$ ($Ln_4 = Sm_4$, Yb_4, Sm_2Yb_2, Nd_2Yb_2)

Deborah Freedman, Safak Sayan, Thomas J. Emge, Mark Croft,[†] and John G. Brennan*

Contribution from the Departments of Chemistry and Physics, Rutgers,
The State University of New Jersey, 610 Taylor Road, Piscataway, New Jersey 08854-8087

Received May 3, 1999

Abstract: The heterovalent ($2 Ln^{2+}$, $2 Ln^{3+}$) tetranuclear $(DME)_4Ln_4Se(SePh)_8$ clusters (Ln = Sm, Yb, Nd-(III)/Yb(II), Sm(III)/Yb(II); DME = dimethoxyethane) can be prepared either by the reduction of Se−C bonds with Ln or by the reaction of $Ln(SePh)_2$ with elemental Se in DME. The Sm(II) compound is difficult to isolate because it slowly redissolves after precipitation. The Yb_4 compound and Nd_2Yb_2 compounds are considerably more stable, and can be isolated in higher yield. For the Ln = Sm_4, Yb_4, Sm_2Yb_2, and Nd_2Yb_2 clusters, low-temperature structural characterization reveals a square array of four metal ions with a crystallographically imposed disorder that renders the Ln(II) and Ln(III) sites indistinguishable; the Nd_2Yb_2 compound also crystallizes in a lattice-solvated unit cell in which there are distinct Ln(II)/Ln(III) metal ions. Connecting the four metals in all structures is a selenido ligand that caps the square array of Ln ions, and pairs of SePh ligands that bridge each of the four edges, with a chelating DME ligand saturating the primary coordination sphere of the seven-coordinate Ln ions. Yb-L_3 X-ray absorption edge measurements on the disordered Yb_4 cluster reveal a strong bimodal white line feature that clearly indicates the presence of both Yb(II) and Yb(III) ions. Magnetic susceptibility measurements on the Yb_4 cluster indicate that the material is a static, inhomogeneous mixed valent material with well-defined Yb(II) and Yb(III) ions and a crossover in the Curie−Weiss behavior at low temperatures is interpreted in terms of crystal field and antiferromagnetic interactions. These small cluster fragments represent intermediates in the stepwise formation of larger clusters, i.e., dimerization of the Ln_4 in a face-to-face arrangement gives the metal core of the now familiar octanuclear $Ln_8E_6(EPh)_{12}$ clusters.

Introduction

There are fundamental reasons for studying the stepwise sequence by which inorganic clusters are assembled from molecular sources. First, there is a considerable effort to understand how the physical properties of solid-state materials depend on the dimensions of the solid, and inorganic clusters are excellent models for mapping out this size dependence, particularly if clusters with well-defined geometries and formulas can be obtained. Second, with an understanding of how particles are assembled, the rational syntheses of complex cluster based materials with select chemical or physical properties can be targeted. Unfortunately, the chemical steps by which stable cluster compounds are assembled from molecular components are rarely illuminated because these intermediate cluster fragments are usually transient species. While the evolution of main group[1] and transition metal[2] cluster systems has been examined in some detail, culminating in the synthesis and structural characterization of clusters as large as $Ag_{172}Se_{40}(Se-n-Bu)_{92}$-$(dppp)_4$,[2g] corresponding studies on the evolution of lanthanide (Ln) systems are relatively undeveloped.

Recent reports of two new and general synthetic approaches to Ln chalcogenido (E, E = S, Se) clusters, i.e., replacement[3] of 2 EPh^- by E^{2-} and reductive cleavage of C−Se bonds,[3a] have supplemented the more conventional ligand redistribution,[4] salt elimination,[5] redox,[6] and alkyl migration[7] routes, thereby enhancing the feasibility of studying the stepwise formation of Ln cluster compounds. This expanded synthetic arsenal increases the likelihood that we will be able to selectively deliver clusters with preordained physical properties or chemical components. For example, in the octanuclear (Lewis base)$_8Ln_8E_6(EPh)_{12}$ compounds, Ln, E, EPh, and Lewis base ligands are each readily

(2) See, for example: (a) Brennan, J.; Siegrist, T.; Stuczynski, S.; Steigerwald, M. *J. Am. Chem. Soc.* **1992**, *114*, 10334. (b) Dahl, L. F.; Johnson, A.; Whoolery, S. *Inorg. Chem. Acta* **1994**, *227*, 269. (c) Fenske, D.; Fischer, A. *Angew. Chem., Int. Ed.* **1995**, *34*, 307. (d) Mathur, P.; Sekar, P. *Chem. Commun.* **1996**, 727. (e) Fenske, D.; Krautscheid, H. *Angew. Chem., Int. Ed.* **1990**, *29*, 1452. (f) Fenske, D.; Corrigan, J. F. *Angew. Chem., Int. Ed.* **1997**, *36*, 1981. (g) Dehnen, S.; Fenske, D. *Angew. Chem., Int. Ed.* **1994**, *33*, 2287. (h) Fenske, D.; Zhu, N.; Langetepe, T. *Angew. Chem., Int. Ed.* **1998**, *37*, 2640.

(3) (a) Freedman, D.; Emge, T. J.; Brennan, J. G. *J. Am. Chem. Soc.* **1997**, *119*, 11112. (b) Freedman, D.; Melman, J.; Emge, T. J.; Brennan, J. G. *Inorg. Chem.* **1998**, *37*, 4162. (c) Melman, J.; Emge, T. J.; Brennan, J. G. *Inorg. Chem.* **1999**, *38*, 2117. (d) Melman, J. H.; Emge, T. J.; Brennan, J. G. *Chem. Commun.* **1997**, 2269. (e) Freedman, D.; Emge, T. J.; Brennan, J. G. *Inorg. Chem.* **1999**, *38*, 4400. (f) Melman, J.; Fitzgerald, M.; Freedman, D.; Emge, T. J.; Brennan, J. G. *J. Am. Chem. Soc.* **1999**, *121*, 10247.

(4) Evans, W.; Rabe, G.; Ziller, J. *Angew. Chem., Int. Ed.* **1994**, *33*, 2110.

(5) Pernin, C. G.; Ibers, J. A. *Inorg. Chem.* **1997**, *36*, 3802.

(6) (a) Berg, D.; Burns, C.; Andersen, R. A.; Zalkin, A. *Organometallics* **1989**, *8*, 1865−70. (b) Evans, W.; Rabe, G.; Ziller, J.; Doedens, R. *Inorg. Chem.* **1994**, *33*, 2719.

(7) Cary, D.; Ball, G.; Arnold, J. *J. Am. Chem. Soc.* **1995**, *117*, 3492.

† Physics Department.

(1) See, for example: (a) Murray, C. B.; Norris, D. J.; Bawendi, M. G. *J. Am. Chem. Soc.* **1993**, *115*, 8706. (b) Herron, N.; Calabrese, J. C.; Farneth, W. E.; Wang, Y. *Science* **1993**, *259*, 1426. (c) Goldstein, A. N.; Escher, C. M.; Alivisatos, A. P. *Science* **1992**, *256*, 1425. (d) Colvin, V. L.; Goldstein, A. N.; Alivisatos, A. P. *J. Am. Chem. Soc.* **1992**, *114*, 5221. (e) Schreiner, B.; Dehnicke, K.; Fenske, D., *Z. Anorg. Allg. Chem.* **1993**, *619*, 1127. (f) Behrens, S.; Fenske, D. *Ber. Bunsen-Ges. Phys.* **1997**, *101*, 1588. (g) Behrens, S.; Bettenhausen, M.; Fenske, D. *Angew. Chem., Int. Ed.* **1998**, *36*, 22797. (h) Fogg, D. E.; Radzilowski, L. H.; Thomas, E. L. *Macromolecules* **1997**, *30*, 417.

controlled synthetic variables.[3e] Such synthetic control permits the determination of structure−property relationships, and from this information we can begin to understand the relationship between particle size and physical properties.

In this work the synthesis and characterization of a series of homologous tetranuclear $(DME)_4Ln_4Se(SePh)_8$ clusters (Ln = Sm (**1**), Yb (**2**), Sm(III)/Yb(II) (**3**), Nd(III)/Yb(II) (**4**); DME = dimethoxyethane) is described. With only one selenido ligand, these compounds represent the earliest possible stage in the synthesis of Ln chalcogenido clusters and solid-state materials from molecular precursors. As such, they are important reference points for understanding the relationship between the physical properties of molecular and solid-state lanthanide compounds.

Experimental Section

General Methods. All syntheses were carried out under ultrapure nitrogen (JWS), using conventional drybox or Schlenk techniques. Solvents (Fisher) were refluxed continuously over molten alkali metals or K/benzophenone and collected immediately prior to use. Anhydrous pyridine (Aldrich) was purchased and refluxed over KOH. PhSeSePh was purchased from either Aldrich or Strem and recrystallized from hexane. Ln and Hg were purchased from Strem. Melting points were taken in sealed capillaries and are uncorrected. IR spectra were taken on a Mattus Cygnus 100 FTIR spectrometer, and recorded from 4000 to 450 cm^{-1} as a Nujol mull on KBr plates. Electronic spectra were recorded on a Varian DMS 100S spectrometer with the samples in a 1 mm quartz cell attached to a Teflon stopcock. Elemental analyses were performed by Quantitative Technologies, Inc. (Whitehouse, NJ). These compounds are moderately sensitive to the thermal dissociation of neutral donor ligands at room temperature and so the experimentally determined elemental analyses are sometimes slightly lower than the computed analyses. Calculated values assume the loss of lattice solvent. Products appear homogeneous, and for every sample several crystals of each compound were examined by single-crystal X-ray diffraction in an attempt to find a crystal suitable for a complete structural determination. The same unit cell was obtained consistently for **1**−**3**, while the Nd/Yb compound was found to crystallize in two different cells (**4′**, **4″**). Magnetic susceptibility was measured on a SQUID magnetometer in a 1 Tesla field. NMR spectra were obtained on either Varian Gemini 200 MHz or Varian 300 or 400 MHz NMR spectrometers and chemical shifts are reported in δ (ppm). Yb-L_3 edge X-ray absorption spectroscopy (XAS) measurements were performed on **2** and standards at beamline X-18B at the Brookhaven National Synchrotron Light Source. A Si(111) channel cut monochromator was used and the data were collected in the fluorescence mode.[8] The samples were sealed in double sets of polyethylene bags under an inert atmosphere and transported to the synchrotron in Schlenk tubes. The XAS measurements were performed on the samples while still sealed in the polyethylene bags. Particular care was taken to minimize the time between the removal from the glass ampule and the data collection. Over a period of 2 h some oxidation was evidenced by an increase of the Yb^{3+} content of the material. The results reported are for the first scan of the material.

Synthesis of $(DME)_4Sm_4Se(SePh)_8\cdot DME$ (1). **Method A:** Samarium powder (0.30 g, 2.0 mmol) was added to a solution of diphenyl diselenide (0.63 g, 2.0 mmol) and mercury (0.05 g, 0.25 mmol) in DME (40 mL). This mixture was stirred for 2 days, then selenium powder (0.079 g, 1.0 mmol) was added to the brown solution and dark green solid. Three days later the dark brown solution was filtered and layered with hexanes (15 mL). After 2 days deep red-black needles (60 mg, 5%; the compound, does not melt, but slowly turned brown and appeared to desolvate at 135 °C, slowly reddened up to 200 °C, and began turning brown again at 288 °C) were isolated. Anal. Calcd for $Sm_4Se_9C_{64}O_8H_{80}$: C, 33.5; H, 3.53. Found: C, 32.9; H, 3.42. IR: 3472 (w), 2925 (s), 2855 (s), 1571 (w), 1462 (s), 1377 (s), 1088 (w), 1065 (w), 1039 (w), 1021 (w), 858 (m), 732 (m), 693 (w), 467 (w) cm^{-1}.

(8) Ramanujachary, K.; Sunstrom, J., IV; Fawcett. I.; Shunk, P.; Greenblatt, M.; Croft, M.; Novik, I.; Herber, R.; Kahalid, S. *Mater. Res. Bull.* **1999**, *34*, 803, and references therein.

The ^1H NMR in OC_4D_8 revealed only displaced DME resonances at 3.43 and 3.27 ppm. λ_{max} (THF): 700 nm ($\epsilon = 9 \times 10^2$ L/(mol·cm), $w_{1/2} = 234$ nm); this absorption band disappears upon addition of Ph_3-PS, thus indicating that the Sm(II) ions can be oxidized readily. **Method B:** Samarium powder (0.30 g, 2.0 mmol) was added to a solution of diphenyl diselenide (0.63 g, 2.0 mmol) in DME (40 mL) and the mixture was stirred at room temperature for 5 days. The dark brown solution was filtered, concentrated slightly (ca. 37 mL), and layered with hexanes (15 mL) to give red-black needles of **1** (ca. 2 mg, 0.2%) that were identified by UV−visible spectroscopy and low-temperature unit cell determination.

Synthesis of $(DME)_4Yb_4Se(SePh)_8\cdot DME$ (2). Ytterbium powder (0.35 g, 2.0 mmol) was added to a mixture of diphenyl diselenide (0.625 g, 2.0 mmol) and mercury (0.05 g, 0.25 mmol) in DME (35 mL). After the mixture was stirred for 3 days, selenium powder (0.08 g, 1 mmol) was added to the dark brown solution and orange solid. The next day the reaction was placed under an atmosphere of hydrogen. After 3 days the dark brown solution was filtered, concentrated to ca. 25 mL, and layered with hexanes (12 mL) to give dark brown crystals (0.12 g, 10%, based on Yb) that do not melt, but begin to desolvate at 118 °C, begin turning black at 210 °C, and turn brown at 285 °C. Anal. Calcd for $Yb_4Se_9C_{64}O_8H_{80}$: C, 32.3; H, 3.39. Found: C, 32.0; H, 3.38. IR: 2925 (s), 1661 (w) 1571 (s), 1461 (s), 1378 (s), 1111 (m), 1089 (m), 1061 (s), 1035 (s), 1020 (s), 862 (s), 828 (w), 732 (s), 693 (s), 664 (m), 467 (m) cm^{-1}. ^1H NMR (OC_4D_8, 27 °C): broad, inseparable resonances at 7.8−6.8 (5 H), 6.48 (3 H), 3.40 (H), 3.25 (H), −5.83 (2 H). λ_{max} (pyridine): 551 nm ($\epsilon = 7 \times 10^2$ L/(mol·cm), $w_{1/2} = 270$ nm). λ_{max} (THF): 422 nm ($\epsilon = 1.2 \times 10^3$ L/(mol·cm)).

Synthesis of $(DME)_4Sm_2Yb_2Se(SePh)_8\cdot DME$ (3). Samarium powder (0.30 g, 2.0 mmol) was added to a mixture of diphenyl diselenide (0.936 g, 3.0 mmol) and mercury (0.05 g, 0.25 mmol) in DME (35 mL). After the mixture was stirred for 2 days ytterbium powder (0.35 g, 2 mmol) was added to the yellow solution and yellow solid. After further stirring for 7 days the red/brown solution was filtered, concentrated to ca. 25 mL, and layered with hexanes (15 mL). Within 2 days dark brown-red crystals had formed (0.15 g, 10%, based on diphenyl diselenide). The compound does not melt, but begins turning orange at ca. 230 °C. Anal. Calcd for $Sm_2Yb_2Se_9C_{64}O_8H_{80}$: C, 32.9; H, 3.46. Found: C, 32.1; H, 3.27. X-ray fluorescence measurements confirm that a 1:1 Nd:Yb ratio is present in the product. IR: 2951 (s), 2870 (s), 2395 (w), 1762 (w), 1571 (m), 1463 (s), 1379 (s), 1238 (w), 1189 (w), 1111 (m), 1089 (m), 1061 (m), 1040 (m), 1020 (m), 901 (w), 859 (s), 826 (m), 732 (s), 692 (s), 662 (w), 523 (w), 468 (m) cm^{-1}. The ^1H NMR spectrum in OC_4D_8 revealed displaced DME resonances and a broad, undefined resonance between 7.0 and 6.4 ppm. λ_{max} (pyridine): 551 nm ($\epsilon = 1 \times 10^3$ L/(mol·cm), $w_{1/2} = 260$ nm).

Synthesis of $(DME)_4Nd_2Yb_2Se(SePh)_8\cdot x$ DME (4). Method A (4″): Ytterbium powder (0.35 g, 2.0 mmol) was added to a mixture of diphenyl diselenide (0.94 g, 3.0 mmol) and mercury (0.05 g, 0.25 mmol) in DME (35 mL). After the mixture was stirred for 2 days Nd powder (0.29 g, 2.0 mmol) was added to the brown solution and tan solid. After 3 days at room temperature and 8 days at 60 °C, the cherry red solution was filtered hot, concentrated to 25 mL, and allowed to sit at room temperature to give red crystals (0.30 g, 19%, based on diphenyl diselenide) that do not melt, but desolvate at 138 °C, gradually turn orange by 212 °C, and turn light brown by 250 °C. Anal. Calcd for $Nd_2Yb_2Se_9C_{64}O_8H_{80}$: C, 33.1; H, 3.48. Found: C, 31.0; H, 3.08. X-ray fluorescence measurements from an entire reaction product and from a 1:1 mixture of Nd/Yb carbonates confirms that there is a 1:1 Nd:Yb ratio present in the product. IR: 2931 (s), 1572 (m), 1461 (s), 1378 (s), 1304 (w), 1279 (w), 1243 (w), 1192 (m), 1114 (s), 1061 (m), 1040 (m), 1022 (m), 939 (w), 856 (s), 734 (s), 693 (m) 663 (w) cm^{-1}. The ^1H NMR spectrum in OC_4D_8 revealed only displaced DME resonances. λ_{max} (pyridine): 551 nm ($\epsilon = 7 \times 10^2$ L/(mol·cm), $w_{1/2} = 260$ nm). λ_{max} (THF): 597 nm ($\epsilon = 7 \times 10^1$ L/(mol·cm), $w_{1/2} = 17$ nm). **Method B (4′):** Neodymium powder (0.29 g, 2.0 mmol) was added to a solution of diphenyl diselenide (0.94 g, 3.0 mmol), in DME (40 mL), and the mixture was stirred for 3 days as a pale blue precipitate formed (Hg can also be added in this reaction to increase the rate of diselenide reduction). Ytterbium powder (0.35 g, 2.0 mmol) was added to the mixture and after being stirred for 6 weeks the cherry red solution was

Heterovalent Clusters: Ln₄Se(SePh)₈

J. Am. Chem. Soc., Vol. 121, No. 50, 1999 11715

Table 1. Summary of Crystallographic Details for $(DME)_4Sm_4Se(SePh)_8 \cdot 1$ DME (**1**), $(DME)_4Yb_4Se(SePh)_8 \cdot 1$ DME (**2**), $(DME)_4Sm_2Yb_2Se(SePh)_8 \cdot 1$ DME (**3**), $(DME)_4Nd_2Yb_2Se(SePh)_8 \cdot 1$ DME (**4′**), and $(DME)_4Nd_2Yb_2Se(SePh)_8 \cdot 2.5$ DME (**4″**)[a]

compd (Ln)₄	**1**	**2**	**3**	**4′**	**4″**
empirical formula	$C_{68}H_{90}O_{10}Se_9Sm_4$	$C_{68}H_{90}O_{10}Se_9Yb_4$	$C_{68}H_{90}O_{10}Se_9Sm_2Yb_2$	$C_{68}H_{90}O_{10}Se_9Nd_2Yb_2$	$C_{74}H_{105}O_{13}Se_9Nd_2Yb_2$
fw	2379.44	2470.2	2424.84	2412.60	2547.78
space group	*P4/ncc* (No. 130)	*P4/ncc* (No. 130)	*P4/ncc* (No. 130)	*P4/ncc* (No. 130)	P4 (No. 75)
a (Å)	18.544(3)	18.289(3)	18.493(3)	18.465(3)	18.831(2)
b (Å)	18.544(3)	18.289(3)	18.493(3)	18.465(3)	18.831(2)
c (Å)	24.015(4)	24.299(14)	24.172(6)	24.100(6)	13.075(2)
α (deg)	90.00(2)	90.00(2)	90.00(2)	90.00(2)	90.00(1)
β (deg)	90.00(2)	90.00(2)	90.00(2)	90.00(2)	90.00(1)
γ (deg)	90.00(2)	90.00(2)	90.00(2)	90.00(2)	90.00(1)
V (Å³)	8258(2)	8128(5)	8267(3)	8217(3)	4637(1)
Z	4	4	4	4	2
D(calcd) (g/cm⁻³)	1.914	2.019	1.948	1.950	1.825
temp (°C)	−120	−120	−120	−120	−120
λ (Å)	0.71073	0.71073	0.71073	0.71073	0.71073
abs coeff (mm⁻¹)	6.82	8.64	7.65	7.53	6.68
no. of total/obsd reflcns	4321/1872	4808/2722	3964/2755	4008/2217	5818/4409
$R(F)$[b] obsd	0.064	0.057	0.037	0.045	0.081
$R_w(F^2)$[b] obsd	0.113	0.120	0.079	0.055	0.208

[a] Additional crystallographic details are given in the Supporting Information. [b] Definitions: $R(F) = \Sigma||F_o| - |F_c||/\Sigma|F_o|$; $R_w(F^2) = \{\Sigma[w(F_o^2 - F_c^2)^2]/\Sigma w(F^{o2})^2\}^{1/2}$; observation criterion: $[I > 2\,\sigma(I)]$.

Table 2. Significant Bond Length Averages (Å) for **1**−**4**

compd	**1**	**2**	**3**	**4′**	**4″** (Nd³⁺/Yb²⁺)
Ln−O	2.52	2.41	2.48	2.49	2.47/2.55
Ln−Se²⁻	2.930	2.833	2.887	2.894	2.887/2.887
Ln−Se(Ph)	3.037	2.958	3.020	3.025	3.023/3.032
Ln−Ln	4.123	3.992	4.070	4.077	4.075, 4.100
Ln ionic radii[19]	1.12	1.01	1.05	1.06	1.04/1.08

filtered, the volume was reduced to ca. 35 mL, and the solution was layered with 15 mL of hexanes to give ca. 2 mg of **4** (identified by UV−vis and X-ray unit cell determination) along with a considerable quantity of amorphous precipitate. The compound crystallizes in two forms [(DME)₄Nd₂Yb₂Se(SePh)₈·1 DME (**4′**) and (DME)₄Nd₂Yb₂Se-(SePh)₈·2.5 DME (**4″**)] that differ primarily in the number of lattice DME molecules contained within the unit cell.

X-ray Structure Determination of 1−4″. Crystals were isolated, immersed in a 1:1 Paratone−mineral oil mixture, mounted onto a glass fiber, and cooled within 5 min. Data for **1**−**4″** were collected on an Enraf-Nonius CAD4 diffractometer with graphite monochromatized Mo Kα radiation ($\lambda = 0.710\ 73$ Å) at −120 °C. The check reflections measured every hour showed less than 2% intensity variation. The data were corrected for Lorenz effects and polarization, and absorption, the latter by a numerical (SHELX76)[9] method. The structures were solved by direct methods (SHELXS86).[10] All non-hydrogen atoms were refined (SHELXL97) based upon F_{obs}^2. All hydrogen atom coordinates were calculated with idealized geometries (SHELXL97).[11] Scattering factors (f_o, f', f'') are as described in SHELXL97. For **4″**, the space group possibilities, from the lack of systematic absences, were *P4*, *P−4*, or *P4/m*. Of these, the *P4* refinement resulted in the lowest $R(F)$ value and the least amount of spatial disorder for both the complex and the DME of solvation. Crystallographic data and final R indices for **1**−**4″** are given in Table 1. Significant bond distance averages for **1**−**4″** are given in Table 2, and significant bond distances and angles for **4″** are given in Table 3. Complete crystallographic details are given in the Supporting Information. An ORTEP diagram[12] of **4″** that also conveys the common structure for **1**−**4′** is shown in Figure 1.

(9) Sheldrick, G. M. SHELX76, Program for Crystal Structure Determination, University of Cambridge, England, 1976.

(10) Sheldrick, G. M. SHELXS86, Program for the Solution of Crystal Structures, University of Göttingen, Germany, 1986.

(11) Sheldrick, G. M. SHELXL97, Program for Crystal Structure Refinement, University of Göttingen, Germany, 1997.

(12) (a) Johnson, C. K. ORTEP II, Report ORNL-5138; Oak Ridge National Laboratory: Oak Ridge, TN, 1976. (b) Zsolnai, L. XPMA and ZORTEP, Programs for Interactive ORTEP Drawings, University of Heidelberg, Germany, 1997.

Results

The cleavage of C−Se bonds by thermally unstable "Sm-(SePh)₂" proceeds at room temperature in DME to give trace yields of deep red (DME)₄Sm₄Se(SePh)₈·DME (**1**) which can be isolated in less than 1% yield (reaction 1). Yield of this cluster

$$\text{"Sm(SePh)}_2\text{"} \xrightarrow{\text{DME, RT, 0.2\% yield}} \text{(DME)}_4\text{Sm}_4\text{Se(SePh)}_8 \quad (1)$$
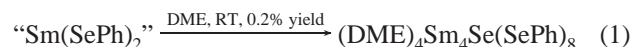
can be improved considerably by addition of elemental Se to the reaction mixture (reaction 2). The compound was character-

$$\text{"Sm(SePh)}_2\text{"} + \text{Se} \xrightarrow{\text{DME, RT, 5\% yield}} \text{(DME)}_4\text{Sm}_4\text{Se(SePh)}_8$$
$$(2)$$
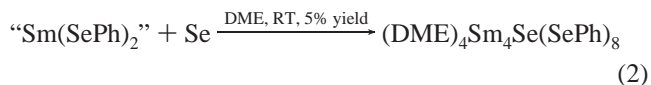
ized by conventional techniques and low-temperature single-crystal X-ray diffraction (Table 1), and average bond distances are listed in Table 2. The structure of **1** consists of a square array of Sm ions, with a Se²⁻ ligand disordered slightly above/below the Sm₄ plane (illustrated with Nd(III) ions and Yb(II) ions in Figure 1). The edges of the square are bridged by pairs of SePh ligands, and the metal coordination sphere is saturated with a chelating DME ligand. While there must be two Sm(II) and two Sm(III) ions per cluster to balance charge, the structure is disordered such that a crystallographically imposed C_4 axis is observed, and the Sm−L bond lengths are intermediate between the distances expected for Sm(II)−L and Sm(III)−L bonds. The crystals are deep red with a broad absorption maximum centered at 710 nm. The isostructural Yb cluster (DME)₄Yb₄Se(SePh)₈·DME (**2**) was also prepared in a stepwise fashion. Reduction of PhSeSePh with Yb in DME gives a solid that has not yet been characterized, but is presumably a DME complex of "Yb(SePh)₂", by analogy with related THF or pyridine coordination complexes of Ln(EPh)ₓ (x = 2, 3).[13,14] This relatively insoluble product reacts with elemental Se to form a brown solution, from which **2** can be isolated. Cluster **2** can be expected to show three allowed electronic transitions, a

(13) (a) Brewer, M.; Khasnis, D.; Buretea, M.; Berardini, M.; Emge, T. J.; Brennan, J. G. *Inorg. Chem.* **1994**, *33*, 2743. (b) Berardini, M.; Emge, T. J.; Brennan, J. G. *J. Am. Chem. Soc.* **1994**, *116*, 6941. (c) Brewer, M.; Lee, J.; Brennan, J. G. *Inorg. Chem.* **1995**, *34*, 5919. (d) Lee, J.; Emge, T. J.; Brennan, J. G. *Inorg. Chem.* **1997**, *36*, 5064.

(14) (a) Lee, J.; Brewer, M.; Berardini, M.; Brennan, J. *Inorg. Chem.* **1995**, *34*, 3215. (b) Lee, J.; Freedman, D.; Melman, J.; Brewer, M.; Sun, L.; Emge, T. J.; Long, F. H.; Brennan, J. G. *Inorg. Chem.* **1998**, *37*, 2512.

Table 3. Significant Bond Lengths (Å) and Angles (deg) for **4″** (Central Se^{2-} Is Se(1))[a]

Yb(1)−O(2)	2.55(3)	Yb(1)−O(1)	2.54(3)	Yb(1)−Se(1)	2.887(3)
Yb(1)−Se(3)	3.002(6)	Yb(1)−Se(4)	3.036(6)	Yb(1)−Se(5)	3.034(7)
Yb(1)−Se(2)	3.054(7)	Nd(1)−O(3)	2.43(3)	Nd(1)−O(4)	2.50(3)
Nd(1)−Se(1)	2.887(2)	Nd(1)−Se(4)′	2.981(7)	Nd(1)−Se(2)	3.009(6)
Nd(1)−Se(3)	3.003(7)	Nd(1)−Se(5)′	3.099(6)		
O(2)−Yb(1)−O(1)	69.0(9)	O(2)−Yb(1)−Se(1)	143.4(8)	O(1)−Yb(1)−Se(1)	147.2(7)
O(2)−Yb(1)−Se(3)	80.1(7)	O(1)−Yb(1)−Se(3)	133.3(6)	Se(1)−Yb(1)−Se(3)	72.9(3)
O(2)−Yb(1)−Se(4)	133.7(7)	O(1)−Yb(1)−Se(4)	79.6(6)	Se(1)−Yb(1)−Se(4)	71.1(3)
Se(3)−Yb(1)−Se(4)	143.8(2)	O(2)−Yb(1)−Se(5)	78.4(7)	O(1)−Yb(1)−Se(5)	98.3(6)
Se(1)−Yb(1)−Se(5)	87.5(2)	Se(3)−Yb(1)−Se(5)	109.1(2)	Se(4)−Yb(1)−Se(5)	73.3(2)
O(2)−Yb(1)−Se(2)	110.1(7)	O(1)−Yb(1)−Se(2)	85.0(6)	Se(1)−Yb(1)−Se(2)	85.6(2)
Se(3)−Yb(1)−Se(2)	73.4(2)	Se(4)−Yb(1)−Se(2)	99.8(2)	Se(5)−Yb(1)−Se(2)	171.5(2)
O(3)−Nd(1)−O(4)	64.3(9)	O(3)−Nd(1)−Se(1)	142.3(8)	O(4)−Nd(1)−Se(1)	152.7(7)
O(3)−Nd(1)−Se(4)′	75.1(7)	O(4)−Nd(1)−Se(4)′	125.4(6)	Se(1)−Nd(1)−Se(4)′	71.9(3)
O(3)−Nd(1)−Se(2)	88.4(7)	O(4)−Nd(1)−Se(2)	103.5(6)	Se(1)−Nd(1)−Se(2)	86.4(2)
Se(4)′−Nd(1)−Se(2)	110.5(2)	O(3)−Nd(1)−Se(3)	140.5(7)	O(4)−Nd(1)−Se(3)	85.4(6)
Se(1)−Nd(1)−Se(3)	72.9(3)	Se(4)′−Nd(1)−Se(3)	144.1(2)	Se(2)−Nd(1)−Se(3)	74.0(2)
O(3)−Nd(1)−Se(5)′	101.3(7)	O(4)−Nd(1)−Se(5)′	80.5(6)	Se(1)−Nd(1)−Se(5)′	86.2(2)
Se(4)′−Nd(1)−Se(5)′	73.2(2)	Se(2)−Nd(1)−Se(5)′	170.2(2)	Se(3)−Nd(1)−Se(5)′	97.7(2)
Nd(1)′−Se−Nd(1)	176.4(8)	Nd(1)′−Se−Yb(1)	90.5(1)	Nd(1)−Se−Yb(1)	89.8(1)
Yb(1)′−Se−Yb(1)	171.3(8)				

[a] Symmetry transformations used to generate equivalent atoms: a prime indicates −x, −y + 1, z.
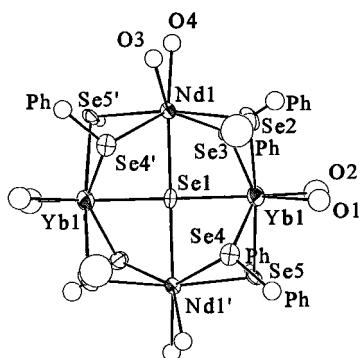
Figure 1. ORTEP diagram of **4″** ((DME)$_4$Nd$_2$Yb$_2$Se(SePh)$_8$) with the C and H atoms removed for clarity. The structures of **1−4′** differ only in that the metal ions are crystallographically disordered such that individual Ln(II) and Ln(III) ions cannot be distinguished.

Se^{2-} to Yb(III) charge transfer (CT) absorption,[3b] a PhSe$^-$ to Yb(III) CT absorption,[14] and an f^{14}-to-f^{13}d^1 promotion,[13a,b] that can explain the intense color of the compound. Unfortunately, because of vibrational broadening these transitions are not resolved in the visible spectrum, and only a single broad absorption centered at 422 nm is observed. Addition of pyridine to **2** results in displacement of the weaker donor solvent by pyridine and the appearance of a resolved absorption maximum at 551 nm that can be assigned as a Yb(II) to py CT absorption, by analogy with Eu(II)[15] and Yb(II)[13a,b] chalcogenolates.

Heterometallic compounds with the same Ln$_4$ framework were also isolated. Trivalent Sm(SePh)$_3$[14b] reacts with elemental Yb, and the resultant red-brown heterometallic Sm(III)/Yb(II) product (DME)$_4$Sm$_2$Yb$_2$Se(SePh)$_8$ (**3**) was found to be isostructural with **1** and **2**. Redox inactive metals are also potential components of this tetranuclear structure: red (DME)$_4$Nd$_2$Yb$_2$-Se(SePh)$_8$ (**4**) can also be prepared, either by the reduction of Yb(SePh)$_3$[14a] with elemental Nd in ca. 20% yield or by the reduction of Nd(SePh)$_3$[14b] with Yb in less than 1% yield (reaction 3). The latter reaction is considerably slower than the former. Both of these Ln(III)/Yb(II) heterometallic products show the same 551 nm Yb to pyridine CT absorption found in the Yb$_4$ cluster, and the electronic transitions responsible for the red colors of **3** and **4** are unresolved in either THF or DME.

For **3**, the 551 nm absorption and the absence of a lower energy band (i.e the 700 nm transition associated with the Sm(II) ion in **1**) are consistent with the Sm(III)/Yb(II) formulation.
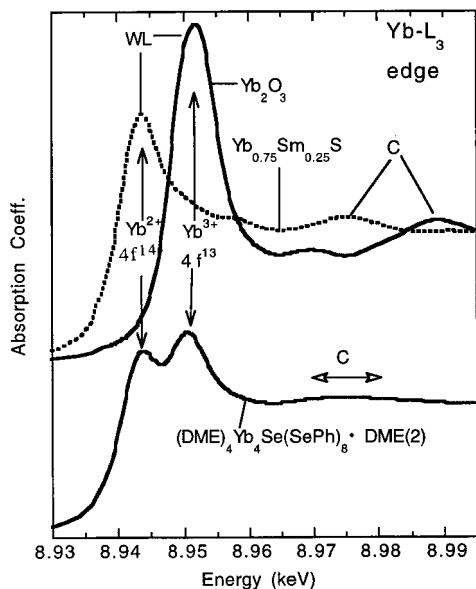
$$4\ Ln(SePh)_3 + 2\ Ln' \xrightarrow{\text{DME}} (DME)_4Ln_2Ln'_2Se(SePh)_8 +$$
$$\text{"PhLn(SePh)}_2\text{"} + \text{"PhLnSe"}\quad (3)$$
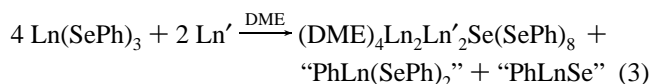
Ln = Nd, Ln′ = Yb, 1% yield; Ln = Yb, Ln′ = Nd,
20% yield

Cluster **4** crystallizes in two unit cells, as determined by low-temperature X-ray diffraction. One cell (**4′**) is isostructural with **1−3**, and the second (**4″**) is a tetragonal space group for which the Nd(III) ions and Yb(II) ions can be distinguished. Table 2 gives a listing of average bond lengths for **1−4′** and **4″**, and significant bond lengths and angles for **4″** are listed in Table 3. From the data in Table 3 it appears that the differences between the Yb(II)−L and Nd(III)−L (L = Se, SePh) bond lengths for each type of bond are slightly less than the differences (0.04 Å) that would be predicted from the ionic radii of Yb(II) and Nd(III). These differences likely result from a compositional disorder of approximately 10%.

Yb-L$_3$ XAS and magnetic susceptibility (χ) measurements were performed on **2** to establish the class of mixed valence compound to which **2** belongs. The XAS measurements (Figure 2) reveal a strong bimodal WL feature that clearly indicates the presence of both Yb(II) and Yb(III) ions, with a slightly greater presence of Yb(III) (56 ± 2%) that can be attributed to partial air oxidation of the sample.[8,16] Magnetic susceptibility measurements of χ vs T were obtained for **2** and are plotted in Figure 3. The χ^{-1} results manifest high- and low-temperature regimes of distinct Curie Weiss (CW) behavior [$\chi = C/(\Theta + T)$].[16] The fitting of the high-temperature CW form is consistent with a full Yb(III) ($J = 7/2$) moment on 50.5% of the sites and no moment on the others.[16] The high- and low-temperature

(15) Berardini, M.; Emge, T.; Brennan, J. G. *J. Am. Chem. Soc.* **1993**, *115*, 8501.

(16) (a) Kemly, E.; Croft, M.; Murgai, V.; Gupta, L. C.; Godart, C.; Parks, R. D.; Segre, C. U. *J. Magn. Magn. Mater.* **1985**, *4748*, 403. (b) Jeon, Y.; F. Lu, F.; Jhans, H.; Shaheen, S. A.; Liang, G.; Croft, M.; Ansari, P. H.; Ramanujachary, K. V.; Hayri, E. A.; Fine, S. M.; Li, X.; Feng, X. H.; Greenblatt, M.; Greene, L. H.; Tarascon, J. M. *Phys. Rev.* **1987**, *B36*, 3891. (c) Ochia, A.; Nakai, S.; Oyamoda, A.; Kasuya, T. *J. Magn. Magn. Mater.* **1985**, *48/7*, 570.

Heterovalent Clusters: Ln₄Se(SePh)₈

J. Am. Chem. Soc., Vol. 121, No. 50, 1999 11717

Figure 2. The Yb-L₃ edges of the Yb^{3+} ($4f^{13}$) standard Yb_2O_3 (top), the Yb^{2+} ($4f^{14}$) standard $Yb_{0.75}Sm_{0.25}S$ (top), and $(DME)_4Yb_4Se(SePh)_8$. The intense "white line" (WL) feature along with its Yb configuration dependent shift are noted in the figure. The weaker *C* features of the spectra are also identified.
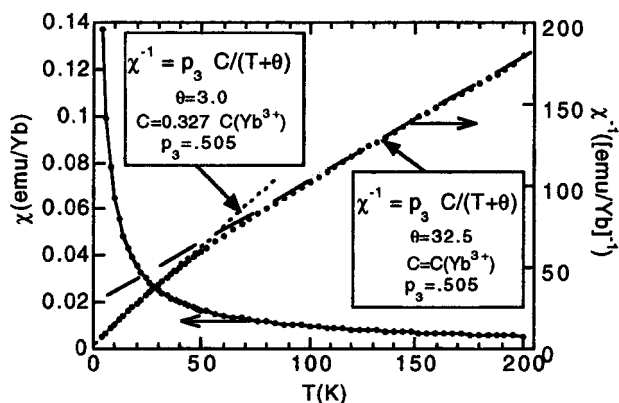
Figure 3. The temperature-dependent magnetic susceptibility (χ) of and its inverse (χ^{-1}) for $(DME)_4Yb_4Se(SePh)_8$.

regimes are consistent with an interplay of antiferromagnetic (AF) and crystalline electric field (CEF) effects.[16,18b–d]

Discussion

The successful isolation of a small cluster fragment is useful for understanding the stepwise formation of larger clusters from molecular precursors. With a variety of $Ln(SePh)_x$ starting materials in DME, both C–Se bond cleavage and redox routes lead to isolation of $(DME)_4Ln_4Se(SePh)_8$. These mixed-valent (Ln(II)/Ln(III)) compounds contain a square array of metal ions with a selenido ligand capping the square face and two SePh ligands connecting adjacent Ln. From the 1–20% isolated yields it is clear that unidentified products also form, but only the Ln₄ cluster has solubility properties that permit isolation from DME. The structure is general for many combinations of Ln(II)/Ln-

(III). However, unlike the $(L)_8Ln_8\,E_6(EPh)_{12}$ cubes that can be isolated with most combinations of Ln, E, EPh, or L,[3a,c–e] the analogous mixed-valent Ln₄ clusters with S^{2-} or benzenethiolate ligands have not yet been successfully isolated.

An analysis of the disordered structures reveals that the observed bond lengths vary with the ionic radii[19] of the component metals, compiled in Table 2. All three bond types, i.e., Ln–O, $Ln–Se^{2-}$, and Ln–Se(Ph), vary in tandem, with the smallest metals showing the smallest average Ln–L bond lengths. Only in the structure of **4″** could distinct Yb(II) and Nd(III) ions be identified, with the individual bond distances given in Table 3. For this compound, the Nd–L bond lengths are within the range of related Nd–O, $Nd–Se^{2-}$, and Nd–Se-(Ph) bond length values found in the $(pyridine)_8Nd_8Se_6(SePh)_{12}$ cluster[3e] or the $[(THF)_4Nd_3(SePh)_9]_n$ coordination polymer.[14b] Similarly, the bond lengths in the homometallic Sm and Yb clusters are within the ranges expected on the basis of related lanthanide selenido/selenolate compounds containing Yb(II),[13a,20] Yb(III),[3b,21] Sm(II),[22] and Sm(III)[3a,e,14b,23] ions that have been structurally characterized.

The Se-capped Ln₄ unit represents a single face of the Ln₈ chalcogenido clusters that form for most of the lanthanides in THF. Dimerization of this cluster would yield the octanuclear Ln_8Se_2 core, with four Sm(II) ions that can subsequently react as pairs of one-electron reducing agents to cleave C–Se bonds and create an additional two Se^{2-} ligands. A ligand redistribution reaction would also be required to produce $Ln_8Se_6(SePh)_{12}$. It is surprising that the Yb₄ compound can be isolated, given that Yb(III) chalcogenido clusters and chalcogenolate complexes have shown a tendency to crystallize with octahedral Yb geometries, i.e., $[(py)_2YbSe(SePh)]_4$,[3b] $(THF)_3Yb(SePh)_3$,[21d] $(DME)Yb(SePh)_4^-$,[21d] $(py)_2Yb(SePh)_4Li(py)_2$,[21a] $(py)_3Yb-(SR)_3$,[14a,24] and $(py)_{10}Yb_6S_6(SPh)_6$.[3b]

Of the three redox-active Ln (Sm, Eu, Yb), only Sm forms an unstable $Ln(SePh)_2$ compound that decomposes thermally by reductively cleaving a C–Se bond, with both Eu and Yb forming isolable coordination compounds. This thermal instability was initially noted in early attempts to prepare coordination complexes of green "$Sm(SePh)_2$".[3a] Eventually solutions of this compound turn red (even in the absence of light), and saturation with apolar solvents gives selenido clusters in isolated yields of up to 42%.[3e] While the thermal decomposition of green Sm-$(SePh)_2$ in DME initially led to **1**, thermolysis is an inferior synthetic approach, presumably because alternative products with Sm–phenyl bonds are also formed. Once elemental Se is added to freshly prepared "$Sm(SePh)_2$", the Sm(II) is oxidized rapidly and cluster **1** can be isolated in yields that permit further experiments.

If left standing in these saturated solutions, crystalline **1** eventually redissolves and the precipitation of an as yet uncharacterized product is observed. The use of DME is key to the precipitation of this small cluster fragment, because the weakly basic, apolar solvent will not solubilize Ln com-

(17) (a) Morrish, A. *The Principles of Magnetism*; John Wiley & Sons: New York, 1965; p 46. (b) Carlin, R. *MagnetoChemistry*; Springer-Verlag: New York, 1986; p 257.

(18) (a) Kasaya, M.; Takigawa, M.; Kasuya, T. *J. Magn. Magn. Mater.* **1985**, *48/7*, 429. (b) Walter, U.; Fisk, Z.; Holland-Moritz, E. *J. Magn. Magn. Mater.* **1985**, *48/7*, 159. (c) Lea, K.; Leask, M.; Wolf, W. *J. Phys. Chem. Solids* **1962**, *23*, 1381. (d) Suryanarayanan, R.; Paparoditis, C.; Ferre, J.; Briat, B. J. *J. Appl. Phys.* **1972**, *43*, 4105.

(19) Shannon, R. D. *Acta Crystallogr. A* **1976**, *32*, 751.

(20) Cary, D. R.; Arnold, J. *Inorg. Chem.* **1994**, *33*, 1791.

(21) (a) Berardini, M.; Emge, T.; Brennan, J. G. *J. Chem. Soc., Chem. Commun.* **1993**, 1537. (b) Wedler, M.; Recknagel, A.; Gilje, J. W.; Noltemeyer, M.; Edelmann, F. T. *J. Organomet. Chem.* **1992**, *426,* 295. (c) Wedler, M.; Noltemeyer, M.; Pieper, U.; Schmidt, H.-G.; Stalke, D.; Edelmann, F. T. *Angew. Chem., Int. Ed.* **1990**, *29*, 894. (d) Geissinger, M.; Magull, J. *Z. Anorg. Allg. Chem.* **1995**, *621*, 2043.

(22) Geissinger, M.; Magull, J. *Z. Anorg. Allg. Chem.* **1997**, *623*, 755.

(23) (a) Taniguchi, Y.; Maruo, M.; Takaki, K.; Fujiwara, Y. *Tetrahedron Lett.* **1994**, *35*, 7789. (b) Mashima, K.; Nakayama, Y.; Nakamura, A.; Kanehisa, N.; Kai, Y.; Takaya, H. *J. Organomet. Chem.* **1994**, *473*, 85.

(24) Mashima, K.; Nakayama, Y.; Fukumoto, H.; Kanehisa, N.; Kai, Y.; Nakamura, A. *J. Chem. Soc., Chem. Commun.* **1994**, 2523.

pounds as effectively as THF, and so cluster compounds that would remain soluble in THF precipitate from DME.

Trivalent $Ln(SePh)_3$ are the preferred starting materials[14] for synthesizing these heterometallic clusters. The heterometallic Nd/Yb compound can be approached by reducing either Ln-$(SePh)_3$ with the second Ln (reaction 3), but the yields clearly indicate that there is an advantage to reducing $Yb(SePh)_3$ with elemental Nd. One possible explanation for this observation is that the first electron reduces the Ln(III), rather than the C−Se bond. Both the relative rates and overall yields of Yb reducing $Nd(SePh)_3$ vs Nd reducing $Yb(SePh)_3$ would be consistent with this hypothesis.

From the limited spectroscopic data that can be obtained, it appears that the Yb compounds remain heterovalent in solution for extended periods of time. For the Yb_4 compound, the NMR spectra indicate that there are at least two inequivalent SePh ligands coordinated to paramagnetic centers. This observation would be consistent with the observed asymmetric structure of the cluster, where the asymmetry is introduced by a Se^{2-} ligand being either above or below the Yb_4 plane. There are no diamagnetic resonances that would suggest the presence of $(THF)_xYb(SePh)_2$ in solution. Significantly, the NMR spectrum does not change over a period of days, indicating that ligand redistribution reactions (i.e., the formation of paramagnetic $(THF)_xYb_nSe_n(SePh)_n$, $(THF)_3Yb(SePh)_3$, and diamagnetic $(THF)_x$-$Yb(SePh)_2$) are either slow or complete within seconds. While the absence of sharp diamagnetic SePh resonances for **2** is evidence against the redistribution process in weaker donor solvents, this stability is not necessarily general for the entire series of clusters, and is better probed with UV−visible spectroscopy for the more paramagnetic clusters.

There are a number of visible absorptions that provide information on the nature of these clusters. The electronic spectra of **2**, **3**, and **4** all have an intense, high-energy absorption band in the UV that tails into the visible spectrum and accounts for the visible color of the clusters both in the solid state and in THF solution. These compounds also exhibit a broad, well-defined Yb−py CT absorption in pyridine[13a,b,15] at 551 nm ($w_{1/2}$ ca. 260 nm) that is nearly identical with the 552 nm absorption reported for $(py)_4Yb(SePh)_2$.[13a]

In contrast, the visible spectrum of the analogous Sm compound **1** has a broad absorption at 700 nm in THF that is not observed when the compound is dissolved in pyridine. More significantly, if **1** is dissolved in pyridine, the anticipated Sm-(II)-to-py CT absorption (this transition should appear at 710 nm, based on relative redox couples[25]) is not observed. These spectroscopic differences can be rationalized by noting that while $Yb(SePh)_2$ coordination compounds appear to be thermally stable in THF with respect to subsequent C−Se bond cleavage reactions, the analogous $Sm(SePh)_2$ compounds are unstable with respect to the formation of Sm(III) selenido clusters,[3a,e] and so the structure of the Sm cluster is not maintained when the compound is dissolved in stronger Lewis base solvents. Analogous Ln(III)/Sm(II) compounds with redox inactive Ln-(III) have not yet been successfully isolated, and so any assignment of the 700 nm (1.7 eV) transition as either an f^6−f^5d^1 promotion[26] or a Sm(II)−Sm(III) CT excitation[27] is tentatively based on data from solid-state literature. In SmSe

there are two f-to-t_{2g} promotions at 1.03 and 1.85 eV,[28] but there are no reports of intermetallic CT in heterovalent Sm_xSe_y. Related measurements on $YbSe_x$ are informative: in YbSe f^{14}-to-$f^{13}t_{2g}^1$ promotions were assigned at 2.05 and 3.0 eV, and a feature at 0.9 eV observed in nonstoichiometric samples was attributed to a Yb(II)−Yb(III) CT process.[26] From these relative excitation energies it is reasonable to suggest that the 700 nm absorption for **1** is a f^6-to-f^5d^1 promotion.

There are also diagnostic electronic absorptions for both **2** and **4**. The Yb_4 compound **2** has a broad absorption centered at 422 nm in THF that may be attributed to some combination of Se to Yb and SePh to Yb(III) charge transfer absorptions. Assignment of this excitation is based on the shift of the corresponding absorptions from the visible to the UV region when a less easily reduced Sm(III) or essentially redox inactive Nd(III) is present. The absence of diagnostic absorptions for $(py)_3Yb(SePh)_3$[3b] or $[(py)_2YbSe(SePh)]_4$[14a] also supports the contention that these clusters do not dissociate in solution. For the Nd/Yb compound **4**, there is also a weak hypersensitive Nd(III) absorption noted in THF at 596 nm that overlaps with the tail of the intense UV absorptions.

The nature of the mixed valence in **2** was probed with Yb-L_3 edge XAS and magnetic susceptibility measurements. L_3 XAS has become a standard technique for estimating the average valence in unstable mixed-valent Ln materials.[8,16] The Ln L_3 edge is dominated by an intense WL feature, due to dipole 2p to 5d transitions (Figure 2). The attractive Coulomb interaction between the 2p-core-hole and the 4f electrons leads to a 7−10 eV shift of the Yb^{3+} ($4f^{13}$) WL feature relative to that of the Yb^{2+} ($4f^{14}$) state (Figure 2).[8] This shift is apparent from the standard spectra in the top of Figure 2. The strongly bimodal Yb-L_3 WL feature, in the spectrum of **2** (Figure 2, bottom), clearly indicates the presence of Yb in both of its configurations with approximately equal weight.[8,16]

It is possible to estimate the relative fraction of the two Yb configurations (valences) present by fitting the spectrum of **2** to two replicate edge features (one for each configuration).[8,16] Such a fit yields the estimated fractional weight of the Yb^{3+} ($4f^{13}$) configuration of $P_3(L_3) = 0.56 \pm 0.02$. Here the error bars in $P_3(L_3)$ reflect uncertainties in the fitting process. Some systematic uncertainties could also arise using different functional forms to model the replicate edge features (here an arc tangent plus a Gaussian was used for each of the replicate features).[8,16] The L_3-determined Yb^{3+} ($4f^{13}$) weight $P_3(L_3) = 0.56$ is in basic agreement with that estimated via the susceptibility below. The somewhat larger Yb^{3+} ($4f^{13}$) content in the L_3-based estimate presumably reflects surface oxidation that is most noticeable for the smallest grains of the sample.

The *C*-features indicated in Figure 2 are due to the photoelectron backscattering from the nearest neighbor ligand shell.[16b] The relatively sharp *C*-features in the integral valent standard spectra (Figure 2, top) reflect the single-edge contribution and single ligand shell distance in these materials.[16b] The broadened *C*-feature in the spectrum of **2** (Figure 2, bottom) is consistent with two replicate edges, with differing ligand shell distances, being superimposed to form the spectrum.

It should be emphasized that the final state Coulomb interaction in this L_3 valence technique renders it incapable of differentiating between inhomogeneous valence mixing (a static array of Yb(II)/Yb(III)) and homogeneous valence mixing (all sites in a fluctuating valence state).[8,16] The magnetic susceptibil-

(25) Bard, A. J.; Parsons, R.; Jordan, J., Ed. *Standard Potentials in Aqueous Solution*; Marcel Decker: New York, 1985.

(26) Lashkarev, G. V.; Ivanchenky, L. A.; Paderno, Y. B. *Phys. Status Solidi B* **1972**, *49*, K61.

(27) Pawlak, L.; Duczmal, M.; Pokryzwnicki, S.; Czopnik, A. *Solid State Commun.* **1980**, *34*, 195.

(28) Suryanarayanan, R.; Paparoditis, C.; Ferre, J.; Briat, B. *J. Appl. Phys.* **1972**, *43*, 4105.

ity results presented below, on the other hand, evidence a static, inhomogeneous valence mixing in this material.

The magnetic susceptibility results manifest high- and low-temperature regimes of distinct Curie–Weiss (CW) behavior [$\chi = C/(T + \theta)$] as indicated by the long and short dashed lines in Figure 3.[17] Fitting high-temperature χ^{-1} data to the CW form (summarized in a box in the figure) yields reduced moment behavior consistent with the fraction of local moment Yb^{3+} sites (p_3) being 0.505. Here these sites are assumed to exhibit a Curie constant $C(Yb^{3+})$ consistent with the full Yb^{3+} ($J = 7/2$) moment ($\mu_{eff} = 4.54$).[17] Within experimental uncertainties the Yb^{3+} fraction is in agreement with the value predicted on the basis of structure and L_3 measurements. The Weiss parameter ($\theta = 32.5$) is presumably related to a combination of antiferromagnetic (AF) interactions and crystalline electric field (CEF) effects.[17] Similar effects have been observed in both cubic Yb_2-Se_3, which also appears to obey the CW law above 100 K ($\theta = 40$, $\mu_{eff} = 4.5$),[26] and the organometallic complex [(C_5Me_5)_2-Yb]_2Se (Yb–Se–Yb = 171.09°), which obeys the CW law above 100 K ($\theta = 15$, $\mu_{eff} = 4.45$),[6a] but the different geometries preclude a detailed analysis of the factors that influence magnetic interactions.

Extensive magnetic susceptibility results in heterovalent solid-state systems have clearly established the signatures of homogeneously mixed valent Yb systems: high-temperature moment reduction followed by a distinct low-temperature maximum in the magnetic susceptibility.[16c,18a,b] There is absolutely no evidence, in the susceptibility results presented here, for the replacement of the low-temperature susceptibility divergence by the characteristic χ maximum.[16c,18a,b] Thus for **2** the magnetic susceptibility and Yb-L_3 edge results provide independent, corroborating evidence of a 1:1 Yb^{3+}/Yb^{2+} mixture; and the χ results mandate that the valence mixing is of the static, inhomogeneous type.[29]

---

(29) Robin, M. B.; Day, P. *Adv. Inorg. Chem. Radiochem.* **1967**, *10*, 248.

The χ cross over, at low temperature, to CW behavior with a reduced Curie constant and Weiss parameter (see Figure 2) is consistent with a crystalline electric field (CEF) effect at the Yb^{3+} sites.[18b–d] Specifically, the strong orbital contribution to the magnetic moments of rare earths invariably leads to the CEF of the ligands splitting the $J = 7/2$ state.[17,18b–d] The temperature scale and magnitude of the low-temperature moment reduction in this material is quite consistent with such a freezing out of a CEF excited state.[18b,d] The residual low-temperature Weiss parameter of $\theta = 3$ K presumably reflects the AF interactions in the CEF ground state.

Conclusions

Homo- and heterotetranuclear lanthanide selenido clusters with the $Ln_4Se(SePh)_8$ formula can be prepared either by reductive cleavage of Se–C bonds or by the reduction of elemental Se by Ln(II) in DME. X-ray absorption spectroscopy and magnetic susceptibility measurements of the $Yb^{II}_2Yb^{III}_2$ compound reveal a static, inhomogeneous mixed-valent material. The Yb(II) compounds maintain some form of heterovalent structure in solution and have electronic absorptions that are indistinguishable from electronic transitions of molecular Yb-(SePh)₂, whereas the Sm(II) compounds decompose at room temperature. These compounds represent an important reference point for relating the properties of molecular and solid-state lanthanide chalcogenido materials.

Supporting Information Available: Fully labeled ORTEP diagrams and a side view of the generic Ln4 structure (PDF) and X-ray crystallographic files for the crystal structures of $(DME)_4Ln_4Se(SePh)_8$ (Ln₄ = Sm₄, Yb₄, Sm₂Yb₂, Nd₂Yb₂) (CIF). This material is available free of charge via the Internet at http://pubs.acs.org.